

# Regression Prior Networks

Andrey Malinin<sup>1,3</sup>, Sergey Chervontsev<sup>1,3</sup>, Ivan Provilkov<sup>1,2</sup>, Mark Gales<sup>4</sup>

<sup>1</sup>Yandex, Moscow, Russia

<sup>2</sup>Moscow Institute of Physics and Technology, Dolgoprudny, Russia

<sup>3</sup>Higher School of Economics, Moscow, Russia

<sup>4</sup>University of Cambridge, Cambridge, UK

{am969, chervontsev, iv-provilkov}@yandex-team.ru, mjfg@eng.cam.ac.uk

## Abstract

Prior Networks are a recently developed class of models which yield interpretable measures of uncertainty and have been shown to outperform state-of-the-art ensemble approaches on a range of tasks. They can also be used to distill an ensemble of models via *Ensemble Distribution Distillation* (EnD<sup>2</sup>), such that its accuracy, calibration and uncertainty estimates are retained within a single model. However, Prior Networks have so far been developed only for classification tasks. This work extends Prior Networks and EnD<sup>2</sup> to regression tasks by considering the Normal-Wishart distribution. The properties of Regression Prior Networks are demonstrated on synthetic data, selected UCI datasets and a monocular depth estimation task, where they yield performance competitive with ensemble approaches.<sup>1</sup>

## 1 Introduction

Neural Networks have become the standard approach to addressing a wide range of machine learning tasks [1, 2, 3, 4, 5, 6, 7, 8, 9, 10]. However, in order to improve the safety of AI systems [11] and avoid costly mistakes in high-risk applications, such as self-driving cars, it is desirable for models to yield estimates of uncertainty in their predictions. Ensemble methods are known to yield both improved predictive performance and robust uncertainty estimates [12, 13, 14]. Importantly, ensemble approaches allow interpretable measures of uncertainty to be derived via a mathematically consistent probabilistic framework. Specifically, the overall *total uncertainty* can be decomposed into *data uncertainty*, or uncertainty due to inherent noise in the data, and *knowledge uncertainty*, which is due to the model having limited uncertainty of the test data [15]. Uncertainty estimates derived from ensembles have been applied to the detection of misclassifications, out-of-domain inputs and adversarial attack detection [16, 17], and active learning [18]. Unfortunately, ensemble methods may be computationally expensive to train and are always expensive during inference.

A class of models called *Prior Networks* [19, 20, 15] was proposed as an approach to modelling uncertainty in classification tasks by *emulating* an ensemble using a *single* model. Prior Networks parameterize a *higher order* conditional distribution over output distributions, such as the Dirichlet distribution. This enables Prior Networks to efficiently yield the same interpretable measures of *total*, *data* and *knowledge uncertainty* as an ensemble. Unlike ensembles, the behaviour of Prior Networks' higher-order distribution is specified via a loss function, such as reverse KL-divergence [20], and training data. However, such Prior Networks yield predictive performance consistent with that of a single model trained via Maximum Likelihood, which is typically worse than that of an ensemble. This can be overcome via Ensemble Distribution Distillation (EnD<sup>2</sup>) [21], which is an approach that allows distilling ensembles into Prior Networks such that measures of ensemble diversity are

<sup>1</sup>Code is available at <https://github.com/JanRocketMan/regression-prior-networks>

preserved. This enables Prior Networks to retain both the predictive performance and uncertainty estimates of an ensemble at low computational and memory cost.

While Prior Networks have many attractive properties, they have only been applied to classification tasks. In this work we develop Prior Networks for *regression tasks* by considering the Normal-Wishart distribution - a higher-order distribution over the parameters of multivariate normal distributions. We derive all measures of uncertainty, the reverse KL-divergence training objective, and the Ensemble Distribution Distillation objective in closed form. Regression Prior Networks are then evaluated on synthetic data, selected UCI datasets and a large scale monocular depth estimation task, where they are shown to yield comparable or better performance to state-of-the-art ensemble approaches.

## 2 Regression Prior Networks

In this section we develop Prior Network models for regression tasks. While typical regression models yield point-estimate predictions, we consider *probabilistic regression models* which parameterizes a distribution  $p(\mathbf{y}|\mathbf{x}, \boldsymbol{\theta})$  over the target  $\mathbf{y} \in \mathcal{R}^K$ . Typically, this is a normal distribution:

$$p(\mathbf{y}|\mathbf{x}, \boldsymbol{\theta}) = \mathcal{N}(\mathbf{y}|\boldsymbol{\mu}, \boldsymbol{\Lambda}), \quad \{\boldsymbol{\mu}, \boldsymbol{\Lambda}\} = \mathbf{f}(\mathbf{x}; \boldsymbol{\theta}) \quad (1)$$

where  $\boldsymbol{\mu}$  is the mean, and  $\boldsymbol{\Lambda}$  the precision matrix, a positive-definite symmetric matrix. While normal distributions are usually defined in terms of the covariance matrix  $\boldsymbol{\Sigma} = \boldsymbol{\Lambda}^{-1}$ , parameterization using the precision tends to be more numerically stable during optimization [22, 23]. While a wide range of distributions over continuous random variables can be considered, we will only use the normal as it makes the least assumptions about the nature of  $\mathbf{y}$  and is mathematically simple.

As in the case for classification, we can consider an ensemble of networks which parameterize multivariate normal distributions  $\{p(\mathbf{y}|\mathbf{x}, \boldsymbol{\theta}^{(m)})\}_{m=1}^M$ . This ensemble can be interpreted as a set of draws from a higher-order implicit distribution over normal distributions. A Prior Network for regression would, therefore, emulate this ensemble by explicitly parameterizing a higher-order distribution over the parameters  $\boldsymbol{\mu}$  and  $\boldsymbol{\Lambda}$  of a normal distribution. One sensible choice is the formidable *Normal-Wishart distribution* [24, 22], which is a conjugate prior to the multivariate normal distribution. This parallels how the Dirichlet distribution, the conjugate prior to the categorical, was used in classification Prior Networks. The Normal-Wishart distribution is defined as follows:

$$\mathcal{NW}(\boldsymbol{\mu}, \boldsymbol{\Lambda}|\mathbf{m}, \mathbf{L}, \kappa, \nu) = \mathcal{N}(\boldsymbol{\mu}|\mathbf{m}, \kappa\boldsymbol{\Lambda})\mathcal{W}(\boldsymbol{\Lambda}|\mathbf{L}, \nu) \quad (2)$$

where  $\mathbf{m}$  and  $\mathbf{L}$  are the *prior mean* and inverse of the positive-definite *prior scatter matrix*, while  $\kappa$  and  $\nu$  are the strengths of belief in each prior, respectively. The parameters  $\kappa$  and  $\nu$  are conceptually similar to *precision* of the Dirichlet distribution  $\alpha_0$ . The Normal-Wishart is a compound distribution which decomposes into a product of a conditional normal distribution over the mean and an Wishart distribution over the precision. Thus, a Regression Prior Network parameterizes the Normal-Wishart distribution over the mean and precision of normal output distributions as follows:

$$p(\boldsymbol{\mu}, \boldsymbol{\Lambda}|\mathbf{x}, \boldsymbol{\theta}) = \mathcal{NW}(\boldsymbol{\mu}, \boldsymbol{\Lambda}|\mathbf{m}, \mathbf{L}, \kappa, \nu), \quad \{\mathbf{m}, \mathbf{L}, \kappa, \nu\} = \boldsymbol{\Omega} = \mathbf{f}(\mathbf{x}; \boldsymbol{\theta}) \quad (3)$$

where  $\boldsymbol{\Omega} = \{\mathbf{m}, \mathbf{L}, \kappa, \nu\}$  is the set of parameters of the Normal-Wishart predicted by neural network. The posterior predictive of this model is the multivariate Student's  $\mathcal{T}$  distribution [24], which is the heavy-tailed generalization of the multivariate normal distribution:

$$p(\mathbf{y}|\mathbf{x}, \boldsymbol{\theta}) = \mathbb{E}_{p(\boldsymbol{\mu}, \boldsymbol{\Lambda}|\mathbf{x}, \boldsymbol{\theta})}[p(\mathbf{y}|\boldsymbol{\mu}, \boldsymbol{\Lambda})] = \mathcal{T}(\mathbf{y}|\mathbf{m}, \frac{\kappa + 1}{\kappa(\nu - K + 1)}\mathbf{L}^{-1}, \nu - K + 1) \quad (4)$$

In the limit, as  $\nu \rightarrow \infty$ , the  $\mathcal{T}$  distribution converges to a normal distribution. The predictive posterior of the Prior Network given in equation 4 only has a defined mean and variance when  $\nu > K + 1$ .

Figure 1 depicts the desired behaviour of an ensemble of normal distributions sampled from a Normal-Wishart distribution. Specifically the ensemble should be consistent for in-domain inputs in regions of low/high *data uncertainty*, as in figures 1a-b, and highly diverse both in the location of the mean and in the structure of the covariance for out-of-distribution inputs, as in figure 1c. Samples of continuous output distributions from a regression Prior Network should yield the same behaviour.

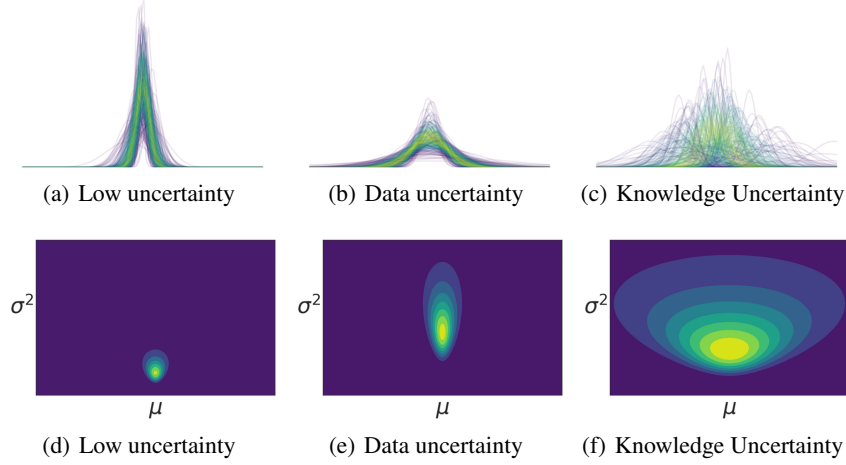


Figure 1: Desired behaviors of an ensemble of regression models. The bottom row displays the desired Normal-Wishart Distribution and the top row depicts Normal Distributions samples from it.

## 2.1 Measures of Uncertainty

Given a Normal-Wishart Prior Network which displays the behaviours above, it is possible to compute closed-form expression for all uncertainty measures previously discussed for ensembles and Dirichlet Prior Networks [15]. By considering the mutual information between the target  $\mathbf{y}$  and the parameters of the output distribution  $\{\boldsymbol{\mu}, \boldsymbol{\Lambda}\}$ , we can obtain measures of *knowledge*, *total* and *data uncertainty*:

$$\underbrace{\mathcal{I}[\mathbf{y}, \{\boldsymbol{\mu}, \boldsymbol{\Lambda}\}]}_{\text{Knowledge Uncertainty}} = \underbrace{\mathcal{H}[\mathbb{E}_{\mathbf{p}(\boldsymbol{\mu}, \boldsymbol{\Lambda}|\mathbf{x}, \boldsymbol{\theta})}[\mathbf{p}(\mathbf{y}|\boldsymbol{\mu}, \boldsymbol{\Lambda})]]}_{\text{Total Uncertainty}} - \underbrace{\mathbb{E}_{\mathbf{p}(\boldsymbol{\mu}, \boldsymbol{\Lambda}|\mathbf{x}, \boldsymbol{\theta})}[\mathcal{H}[\mathbf{p}(\mathbf{y}|\boldsymbol{\mu}, \boldsymbol{\Lambda})]]}_{\text{Expected Data Uncertainty}} \quad (5)$$

This expression consists of the difference between the differential entropy of the posterior predictive and the expected differential entropy of draws from the Normal-Wishart prior. We can also consider the *expected pairwise KL-divergence* (EPKL) between draws from the Normal-Wishart prior:

$$\mathcal{K}[\mathbf{y}, \{\boldsymbol{\mu}, \boldsymbol{\Lambda}\}] = -\mathbb{E}_{\mathbf{p}(\mathbf{y}|\mathbf{x}, \boldsymbol{\theta})}[\mathbb{E}_{\mathbf{p}(\boldsymbol{\mu}, \boldsymbol{\Lambda}|\mathbf{x}, \boldsymbol{\theta})}[\ln \mathbf{p}(\mathbf{y}|\boldsymbol{\mu}, \boldsymbol{\Lambda})]] - \mathbb{E}_{\mathbf{p}(\boldsymbol{\mu}, \boldsymbol{\Lambda}|\mathbf{x}, \boldsymbol{\theta})}[\mathcal{H}[\mathbf{p}(\mathbf{y}|\boldsymbol{\mu}, \boldsymbol{\Lambda})]] \quad (6)$$

This is an upper bound on mutual information [15]. Notably, estimates of data uncertainty are unchanged. One practical use of EPKL is comparison with ensembles, as it is not possible to obtain a tractable expression for the mutual information of a regression ensemble [15]. Alternatively, we can consider measures of uncertainty derived via the law of total variance:

$$\underbrace{\mathbb{V}_{\mathbf{p}(\boldsymbol{\mu}, \boldsymbol{\Lambda}|\mathbf{x}, \boldsymbol{\theta})}[\boldsymbol{\mu}]}_{\text{Knowledge Uncertainty}} = \underbrace{\mathbb{V}_{\mathbf{p}(\mathbf{y}|\mathbf{x}, \boldsymbol{\theta})}[\mathbf{y}]}_{\text{Total Uncertainty}} - \underbrace{\mathbb{E}_{\mathbf{p}(\boldsymbol{\mu}, \boldsymbol{\Lambda}|\mathbf{x}, \boldsymbol{\theta})}[\boldsymbol{\Lambda}^{-1}]}_{\text{Expected Data Uncertainty}} \quad (7)$$

This yields a similar decomposition to mutual information, but only first and second moments are considered. We provide closed-form expressions of (5)-(7) in appendix A. We omit the closed-form expressions for all terms here and instead provide them in appendix A.

## 2.2 Training objectives

Having discussed how to construct Prior Networks for regression, we now discuss how they can be trained. Prior Networks are trained using a multi-task loss, where an in-domain loss  $\mathcal{L}_{in}$  and an out-of-distribution (OOD) loss  $\mathcal{L}_{out}$  are jointly minimized:

$$\mathcal{L}(\boldsymbol{\theta}, \mathcal{D}_{tr}, \mathcal{D}_{out}) = \mathbb{E}_{\mathbf{p}_{tr}(\mathbf{y}, \mathbf{x})}[\mathcal{L}_{in}(\mathbf{y}, \mathbf{x}, \boldsymbol{\theta})] + \gamma \cdot \mathbb{E}_{\mathbf{p}_{out}(\mathbf{x})}[\mathcal{L}_{out}(\mathbf{x}, \boldsymbol{\theta})] \quad (8)$$

The OOD loss is necessary to teach the model the limit of its knowledge [15]. Normal distributions sampled from a Prior Network should be consistent and reflect the correct level of *data uncertainty* in-domain, and diverse in both mean and precision out-of-domain. Achieving the former is challenging,

as the training data only consists of samples of inputs  $\mathbf{x}$  and targets  $\mathbf{y}$ , there is no access to the underlying distribution, and associated data uncertainty, represented by the precision  $\mathbf{\Lambda}$ . Effectively, we are attempting to train a Normal-Wishart distribution from targets sampled from normal distribution that are sampled from the Normal-Wishart, rather than on the normal distribution samples themselves, which is challenging. However, it was shown that for Dirichlet Prior Networks minimizing the *reverse* KL-divergence between the model and an appropriate target Dirichlet *induces in expectation* the correct estimate of *data uncertainty* [20]. As the Normal-Wishart, like the Dirichlet, is a conjugate prior and exponential family member, the precision can be *induced in expectation* by considering the *reverse* KL-divergence between the model  $p(\boldsymbol{\mu}, \mathbf{\Lambda}|\mathbf{x}, \boldsymbol{\theta})$  and a target Normal-Wishart  $p(\boldsymbol{\mu}, \mathbf{\Lambda}|\hat{\boldsymbol{\Omega}}^{(i)})$  corresponding to each  $\mathbf{x}^{(i)}$ . The appropriate Normal-Wishart is specified via Bayes's rule:

$$p(\boldsymbol{\mu}, \mathbf{\Lambda}|\hat{\boldsymbol{\Omega}}^{(i)}) \propto p(\mathbf{y}^{(i)}|\boldsymbol{\mu}, \mathbf{\Lambda})^{\hat{\beta}} p(\boldsymbol{\mu}, \mathbf{\Lambda}|\boldsymbol{\Omega}_0) \quad (9)$$

where  $\boldsymbol{\Omega}_0 = \{\mathbf{m}_0, \mathbf{L}_0, \kappa_0, \nu_0\}$  are the parameters of the prior defined as follows:

$$\mathbf{m}_0 = \frac{1}{N} \sum_{i=1}^N \mathbf{y}^{(i)}, \mathbf{L}_0^{-1} = \frac{\nu_0}{N} \sum_{i=1}^N (\mathbf{y}^{(i)} - \mathbf{m}_0)(\mathbf{y}^{(i)} - \mathbf{m}_0)^T, \kappa_0 = \epsilon, \nu_0 = K + 1 + \epsilon \quad (10)$$

In other words, we consider a *semi-informative prior* which corresponds to the mean and scatter matrix of marginal distribution  $p(\mathbf{y})$ , and we see each sample of the training data  $\hat{\beta}$  times. The hyper-parameter  $\hat{\beta}$  allows us to weigh the effect of the prior and the data.  $\epsilon$  is a small value, like  $10^{-2}$ , so that  $\kappa_0$  and  $\nu_0$  yield a maximally un-informative, but proper predictive posterior. The reason to use a semi-informative prior is because in regression tasks, unlike classification tasks, uninformative priors are improper and lead to infinite differential entropy. Furthermore, we do know *something* about the data purely based on the marginal distribution, and it is sensible to use that as the prior. The reverse KL-divergence loss can then be expressed as:

$$\begin{aligned} \mathcal{L}(\mathbf{y}, \mathbf{x}, \boldsymbol{\theta}; \hat{\beta}, \boldsymbol{\Omega}_0) &= \text{KL}[p(\boldsymbol{\mu}, \mathbf{\Lambda}|\mathbf{x}, \boldsymbol{\theta})||p(\boldsymbol{\mu}, \mathbf{\Lambda}|\hat{\boldsymbol{\Omega}}^{(i)})] \\ &= \hat{\beta} \cdot \mathbb{E}_{p(\boldsymbol{\mu}, \mathbf{\Lambda}|\mathbf{x}, \boldsymbol{\theta})} [-\ln p(\mathbf{y}|\boldsymbol{\mu}, \mathbf{\Lambda})] + \text{KL}[p(\boldsymbol{\mu}, \mathbf{\Lambda}|\mathbf{x}, \boldsymbol{\theta})||p(\boldsymbol{\mu}, \mathbf{\Lambda}|\boldsymbol{\Omega}_0)] + Z \end{aligned} \quad (11)$$

where  $Z$  is a normalization constant. For in-domain data  $\hat{\beta}$  can be set to a large value, and for out-of-domain training data  $\hat{\beta} = 0$ , so that the model regresses to the prior. In-domain the prior will add a degree of smoothing which may prevent over-fitting and improve performance on small datasets. The derivation and closed form expression for this loss is provided in appendix A.

### 2.3 Ensemble Distribution Distillation

An interesting task which Prior Networks can solve is *Ensemble Distribution Distillation* (EnD<sup>2</sup>) [21], where the distribution of an ensemble's predictions is distilled into a single model. EnD<sup>2</sup> enables retaining an ensemble's improved predictive performance and uncertainty estimates within a single model at low cost. In contrast, standard Ensemble Distillation (EnD), which minimizes the KL-divergence between a model and the ensemble posterior, loses information about ensemble diversity.

Consider an ensemble  $\{p(\mathbf{y}|\mathbf{x}, \boldsymbol{\theta}^{(m)})\}_{m=1}^M$ , where each model yields the mean and precision of a normal distribution. We can define an empirical distribution over the mean and precision as follows:

$$\hat{p}(\boldsymbol{\mu}, \mathbf{\Lambda}, \mathbf{x}) = \{\{\boldsymbol{\mu}^{(mi)}, \mathbf{\Lambda}^{(mi)}\}_{m=1}^M, \mathbf{x}^{(i)}\}_{i=1}^N = \mathcal{D}_{trn} \quad (12)$$

EnD<sup>2</sup> can then be accomplished by minimizing the negative log-likelihood of the ensemble's mean and precision under the Normal-Wishart prior:

$$\mathcal{L}(\phi, \mathcal{D}_{trn}) = \mathbb{E}_{\hat{p}(\boldsymbol{\mu}, \mathbf{\Lambda}, \mathbf{x})} [-\ln p(\boldsymbol{\mu}, \mathbf{\Lambda}|\mathbf{x}; \phi)] = \mathbb{E}_{\hat{p}(\mathbf{x})} [\text{KL}[\hat{p}(\boldsymbol{\mu}, \mathbf{\Lambda}|\mathbf{x})||p(\boldsymbol{\mu}, \mathbf{\Lambda}|\mathbf{x}; \phi)]] + Z \quad (13)$$

This is equivalent to minimizing the KL-divergence between the model and the empirical distribution of the ensemble. Note that here, unlike in the previous section, the parameters of a normal distribution are available for every input  $\mathbf{x}$ , making forward KL-divergence the appropriate loss function. However, while this is a theoretically sound approach, the optimization might be numerically challenging. Similarly to [21] we propose a temperature-annealing trick to make the optimization process easier.

First, the ensemble is reduced to it's mean:

$$\begin{aligned}\mu_T^{(mi)} &= \frac{2}{T+1}\mu^{(mi)} + \frac{T-1}{T+1}\bar{\mu}^{(i)}, \quad \bar{\mu}^{(i)} = \frac{1}{M}\sum_{m=1}^M \mu^{(mi)} \\ \Lambda_T^{-1(mi)} &= \frac{2}{T+1}\Lambda^{-1(mi)} + \frac{T-1}{T+1}\bar{\Lambda}^{-1(i)}, \quad \bar{\Lambda}^{-1(i)} = \frac{1}{M}\sum_{m=1}^M \Lambda^{-1(mi)}\end{aligned}\tag{14}$$

In the expression above we use inverses of the precision matrix  $\Lambda$  because we are actually interpolating the covariance matrices  $\Sigma$ . Secondly, the predicted  $\tilde{\kappa} = T\kappa$  and  $\tilde{\nu} = T\nu$  are multiplied by  $T$  in order to make the Normal-Wishart also sharp around the mean. The loss is *divided* by  $T$  in order to avoid scaling the gradients by  $T$ , yielding:

$$\begin{aligned}\mathbf{p}_T(\mu, \Lambda | \mathbf{x}, \phi) &= \mathcal{NW}(\mu, \Lambda | \mathbf{m}, \mathbf{L}, T\kappa, T\nu), \quad \{\mathbf{m}, \mathbf{L}, \kappa, \nu\} = \mathbf{f}(\mathbf{x}; \phi) \\ \mathcal{L}(\phi, \mathcal{D}_{trn}; T) &= \frac{1}{T}\mathbb{E}_{\mathbf{p}_T(\mu, \Lambda, \mathbf{x})}[-\ln \mathbf{p}_T(\mu, \Lambda | \mathbf{x}; T, \phi)]\end{aligned}\tag{15}$$

This splits learning into two phases. First, when temperature is high, the model learns to match the ensemble's mean (first moment). Second, as the temperature is annealed down to 1, the model will gradually focus on learning higher moments of the ensemble's distribution. This trick may be necessary, as the ensemble may have a highly non-Normal-Wishart distribution, which may be challenging to learn. Finally, note that for EnD<sup>2</sup> it may be better to parameterize the *Normal-inverse-Wishart* distribution over the mean and covariance, due to numerical stability concerns. However, for consistency, we describe EnD<sup>2</sup> in terms of the Normal-Wishart.

### 3 Experiments on synthetic data

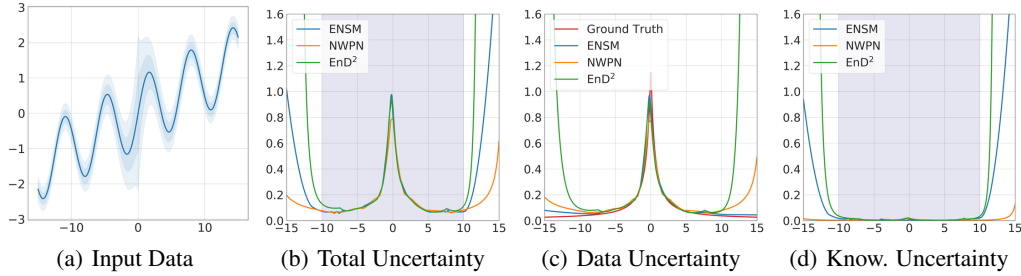


Figure 2: Comparison of different models on synthetic data  $y \sim \mathcal{N}(\sin x + \frac{x}{10}, \frac{1}{|x|+1} + 0.01)$ . Gray area indicates training data region.

We first examine Regression Prior Networks on a synthetic one-dimensional dataset with additive heteroscedastic noise. We compare Regression Prior Network trained via RKL (NWP) and distribution-distillation of an ensemble (EnD<sup>2</sup>) to Deep Ensembles. The ensemble consists of 10 models which yield a Normal output distribution and are trained via maximum likelihood. All models use the same 2-layer architecture with 30 ReLU units. Details of the setup are available in appendix B. The NWP was trained via reverse KL-divergence (11) and Ensemble Distribution Distillation done as described in section 2.3. In-domain training data for all models is sampled between  $[-10, 10]$  and OOD training data for the NWP model is sampled from  $[-25, 20] \cup [20, 25]$ . Measures of *total*, *data* and *knowledge uncertainty* are obtained via the law of total variance (7).

The results presented in Figure 2 show several trends. Firstly, the total uncertainty of all models is high in the region of high heteroscedastic noise as well as out-of-domain. Secondly, *total uncertainty* decomposes into *data uncertainty* and *knowledge uncertainty*. The former is high in the region of high heteroscedastic noise and has undefined behaviour out-of-domain, while the latter is low in-domain and large out-of-distribution. Third, EnD<sup>2</sup> successfully replicates ensemble's estimates of uncertainty, though they are consistently larger, especially estimates of *data uncertainty* out-of-domain. This is a consequence of the ensemble being non-Normal-Wishart distributed when it is diverse, leading the EnD<sup>2</sup> Prior Network to over-estimate support. Thus, these results validate the principle claims that Regression Prior Networks can emulate the behaviour of an ensemble via multi-task training using the RKL objective or via EnD<sup>2</sup>, and that they yield interpretable measures of uncertainty.

## 4 Experiments on UCI data

In this section we evaluate Normal-Wishart Prior Networks trained via reverse-KL divergence (11) (NWPN) and Ensemble Distribution Distillation (EnD<sup>2</sup>) relative to a Deep-Ensemble baseline on selected UCI datasets. Other ensemble-methods are not considered, as Deep Ensemble have been shown to consistently outperform them using fewer ensemble members [25, 26, 27]. Results on remaining UCI datasets are available in appendix C. We follow the experimental setup of [13] with several changes, detailed in appendix C. Out-of-distribution training data for Prior Networks trained via RKL is generated using factor analysis with increased noise and latent variance as in [15]. Table 1 shows a comparison of all models in terms of NLL and RMSE. Unsurprisingly, ensembles yield the best RMSE, though both NWPN and EnD<sup>2</sup> give generally comparable NLL scores. Furthermore, EnD<sup>2</sup> comes close to or matches the performance of the ensemble and outperforms NWPN. This is expected, as NWPN is a single model trained with RKL, which is an upper-bound on NLL.

Table 1: RMSE and NLL of models on UCI datasets. Datasets listed in order of increasing size.

Data	RMSE ( $\downarrow$ )				NLL ( $\downarrow$ )			
	Single	ENSM	EnD <sup>2</sup>	NWPN	Single	ENSM	EnD <sup>2</sup>	NWPN
wine	$0.65 \pm 0.01$	<b><math>0.63 \pm 0.01</math></b>	<b><math>0.63 \pm 0.01</math></b>	<b><math>0.63 \pm 0.01</math></b>	$1.24 \pm 0.16$	$0.96 \pm 0.03$	<b><math>0.91 \pm 0.02</math></b>	$0.93 \pm 0.02$
power	$4.07 \pm 0.07$	<b><math>4.00 \pm 0.07</math></b>	$4.06 \pm 0.07$	$4.09 \pm 0.07$	$2.82 \pm 0.02$	<b><math>2.79 \pm 0.02</math></b>	<b><math>2.79 \pm 0.01</math></b>	$2.81 \pm 0.01$
MSD	$9.08 \pm 0.00$	<b><math>8.92 \pm 0.00</math></b>	$8.94 \pm 0.00$	$9.07 \pm 0.00$	$3.51 \pm 0.00$	<b><math>3.39 \pm 0.00</math></b>	<b><math>3.39 \pm 0.00</math></b>	$3.41 \pm 0.00$

In Table 2 we compare uncertainty measures derived from all models on the tasks of error detection and OOD detection, which are evaluated using Prediction Rejection Ratio (PRR) [21, 15] and AUC-ROC [28], respectively. Finding ‘real’ out-of-domain data for UCI datasets is challenging, so we construct a synthetic OOD dataset for an in-domain UCI dataset with  $K$  columns by taking first  $K$  non-constant columns from a *different* UCI dataset. Columns of each OOD dataset are normalized using statistics derived from the in-domain training dataset. Details are available in appendix C.

The results show that all models achieve comparable error-detection using measures of *total uncertainty*. In terms of OOD detection, EnD<sup>2</sup> generally reproduces the ensemble’s behaviour, while NWPN usually performs worse. However, on the MSD dataset NWPN yields the best performance. This may be due to the nature of the OOD training data - it may simply be better suited to MSD OOD detection. Furthermore, the UCI datasets are generally small and have low input dimensionality - MSD, the largest, has 95 features. It is therefore difficult to assess the superiority of any particular model on these simple datasets - all we can say that they generally perform comparably. A more complex, larger-scale, task is required to properly validate regression Prior Networks.

Table 2: PRR and OOD detection scores

Data	Model	PRR ( $\uparrow$ )		AUC-ROC ( $\uparrow$ )		
		$\mathcal{H}[\mathbb{E}]$	$\mathbb{V}[y]$	$\mathcal{I}$	$\mathcal{K}$	$\mathbb{V}[\mu]$
wine	ENSM	-	<b><math>0.32 \pm 0.02</math></b>	-	$0.58 \pm 0.01$	$0.56 \pm 0.02$
	EnD <sup>2</sup>	$0.30 \pm 0.02$	$0.30 \pm 0.02$	<b><math>0.65 \pm 0.01</math></b>	<b><math>0.65 \pm 0.01</math></b>	<b><math>0.65 \pm 0.03</math></b>
	NWPN	$0.30 \pm 0.03$	$0.30 \pm 0.03$	$0.64 \pm 0.01$	$0.64 \pm 0.01$	$0.53 \pm 0.02$
power	ENSM	-	<b><math>0.23 \pm 0.01</math></b>	-	$0.64 \pm 0.02$	$0.62 \pm 0.02$
	EnD <sup>2</sup>	<b><math>0.23 \pm 0.01</math></b>	<b><math>0.23 \pm 0.01</math></b>	<b><math>0.66 \pm 0.01</math></b>	<b><math>0.66 \pm 0.01</math></b>	$0.50 \pm 0.02$
	NWPN	$0.20 \pm 0.02$	$0.20 \pm 0.02$	$0.56 \pm 0.01$	$0.56 \pm 0.01$	$0.31 \pm 0.02$
msd	ENSM	-	<b><math>0.64 \pm 0.00</math></b>	-	$0.55 \pm 0.0$	$0.62 \pm 0.0$
	EnD <sup>2</sup>	$0.63 \pm 0.00$	$0.63 \pm 0.00$	$0.50 \pm 0.0$	$0.50 \pm 0.0$	$0.65 \pm 0.0$
	NWPN	<b><math>0.64 \pm 0.00</math></b>	<b><math>0.64 \pm 0.00</math></b>	$0.73 \pm 0.0$	$0.73 \pm 0.0$	<b><math>0.75 \pm 0.0</math></b>

## 5 Monocular Depth Estimation Experiments

Having established that the proposed methods work on par with or better than ensemble methods on the UCI datasets, we now examine them on the large-scale NYU Depth v2 depth-estimation task [29].

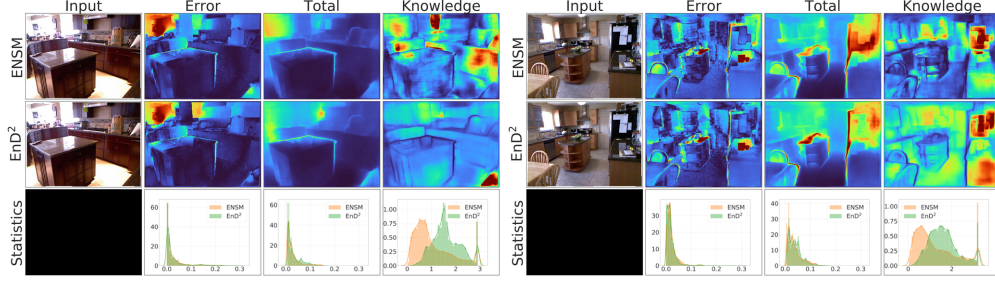


Figure 3: Comparison of uncertainty measures between ensembles and EnD<sup>2</sup>.

We highlight that we *do not* aim for state-of-the-art performance. Rather, the aim is to demonstrate that Ensemble Distribution Distillation using Regression Prior Networks is a general technique which allows a single model to retain the benefits of an ensemble. As a baseline, we take DenseDepth model (DD) which defines a U-Net like architecture on top of DenseNet-169 features [30]. The original approach trains it on inverted targets using a combination of L1, SSIM and Image-Gradient losses. We replace this with NLL training using a model which yields mean and precision for each pixel (Single). The data pre-processing, augmentation, optimization and evaluation protocol are kept unchanged. Surprisingly, table 3 shows that this improves performance.

Table 3: Predictive Performance comparison

Method	$\delta_1(\uparrow)$	$\delta_2(\uparrow)$	$\delta_3(\uparrow)$	rel( $\downarrow$ )	rmse( $\downarrow$ )	$\log_{10}(\downarrow)$	NLL( $\downarrow$ )
DD	0.847 $\pm$ NA	0.972 $\pm$ NA	0.993 $\pm$ NA	0.124 $\pm$ NA	0.468 $\pm$ NA	0.054 $\pm$ NA	-
ENSM 5	<b>0.862</b> $\pm$ NA	<b>0.975</b> $\pm$ NA	<b>0.994</b> $\pm$ NA	<b>0.117</b> $\pm$ NA	<b>0.438</b> $\pm$ NA	<b>0.051</b> $\pm$ NA	0.76 $\pm$ NA
Single	0.853 $\pm$ 0.002	0.971 $\pm$ 0.001	0.993 $\pm$ 0.000	0.122 $\pm$ 0.001	0.455 $\pm$ 0.003	0.053 $\pm$ 0.000	5.93 $\pm$ 1.72
EnD	0.851 $\pm$ 0.003	0.971 $\pm$ 0.000	0.993 $\pm$ 0.000	0.122 $\pm$ 0.001	0.457 $\pm$ 0.004	0.053 $\pm$ 0.000	9.11 $\pm$ 2.65
EnD <sup>2</sup> <sub>T=1</sub>	0.855 $\pm$ 0.004	0.972 $\pm$ 0.001	0.993 $\pm$ 0.000	0.120 $\pm$ 0.001	0.451 $\pm$ 0.007	0.052 $\pm$ 0.001	-1.43 $\pm$ 0.02
EnD <sup>2</sup> <sub>T=10</sub>	0.855 $\pm$ 0.002	0.972 $\pm$ 0.001	0.993 $\pm$ 0.000	0.121 $\pm$ 0.001	0.451 $\pm$ 0.003	0.052 $\pm$ 0.001	<b>-1.47 <math>\pm</math> 0.06</b>

A Deep-Ensemble of 5 Gaussian models (ENSM) is constructed and distribution-distilled into a Regression Prior Network (EnD<sup>2</sup>) with a per-pixel Normal-Wishart distribution. Other ensemble-methods are not considered, as Deep Ensembles consistently outperform them [25, 26]. We also consider standard ensemble distillation (EnD). All experiments are repeated 4 times and we report mean and standard deviation of the results in table 3. We perform an ablation study and examine the effect of temperature annealing ( $T = 1.0$  vs.  $T = 10.0$ ). For  $T = 10.0$  we use the following schedule: train with initial temperature for 20% of epochs, linearly decay it to 1.0 during 60% of epochs, fine-tune with  $T = 1.0$  for the last 20% of epochs. Results in table 3 show that EnD<sup>2</sup> achieves performance closer to that of an ensemble. Using a temperature annealing schedule with an initial temperature of 10 provides marginal improvements and makes the results more consistent. This suggests that the curriculum learning introduced by temperature annealing is useful, but not as critical as it is for classification EnD<sup>2</sup> [21]. Additionally, we assess calibration in terms of test-set NLL. Surprisingly, EnD<sup>2</sup> yields predictions which are better calibrated than ensembles. Temperature annealing provides a further improvement. This may be due to the ensemble being poorly modelled by a Normal-Wishart distribution, leading the Prior Network to over-estimate the support of the distribution. As a consequence, the EnD<sup>2</sup> is less confident, and therefore better calibrated. In contrast, EnD has significantly worse calibration than even a single models.

Figure 3 shows the error and estimates of *total* and *knowledge uncertainty* yielded by an ensemble and an EnD<sup>2</sup> model for the same input image. Clearly, both the ensemble and our model effectively decompose uncertainty. *Total uncertainty* is large at object boundaries and distant points while *knowledge uncertainty* concentrates on the interior of unusual objects. EnD<sup>2</sup> yields both error and measures of uncertainty which are very similar to that of the original ensemble. This demonstrates that EnD<sup>2</sup> is able to emulate not only the predictive performance of the ensemble, but also the behaviour of the ensemble’s measures of uncertainty. Additional comparisons are provided in appendix D.

In table 4 we asses all models on the task of out-of-domain input detection. Three OOD test-datasets are considered: KITTI [31], LSUN-church (LSN-C) and LSUN-bed (LSN-B) [32], which consists of images of general scenes, churches and bedrooms. The latter is most similar to NYU Depth-V2 and more challenging to detect. OOD images are center-cropped and re-scaled to the  $480 \times 640$  resolution of NYU. There are several notable trends. Firstly, EnD<sup>2</sup> consistently outperforms the original ensemble using measures of *knowledge uncertainty* ( $\mathcal{I}$ ,  $\mathcal{K}$  and  $\mathbb{V}[\mu]$ ). However, when considering measures of *total uncertainty* ( $\mathcal{H}[\mathbb{E}]$ ,  $\mathbb{V}[\mathbf{y}]$ ), the ensemble tends to yield superior performance. This is likely due to over-estimation of the support of the ensemble’s distribution by EnD<sup>2</sup>. Secondly, OOD detection is easier on more-mismatched datasets. Temperature annealing both improve performance and make it more consistent. Curiously, standard ensemble distillation (EnD) does much worse than even a single model, which was an effect that was also observed for classification models in [21]. Finally, variance-based measures consistently outperform information-theoretic measures of *total uncertainty*, and sometimes *knowledge uncertainty*.

Table 4: OOD detection % AUC-ROC ( $\uparrow$ ) comparison

Method	OOD	$\mathcal{H}[\mathbb{E}]$	$\mathbb{V}[\mathbf{y}]$	$\mathcal{I}$	$\mathcal{K}$	$\mathbb{V}[\mu]$
Single	LSN-B	$0.734 \pm 0.004$	$0.734 \pm 0.004$	-	-	-
ENSM		-	$0.773 \pm \text{NA}$	-	$0.725 \pm \text{NA}$	$0.798 \pm \text{NA}$
EnD		$0.674 \pm 0.022$	$0.674 \pm 0.022$	-	-	-
EnD <sup>2</sup> , $T = 1.0$		$0.783 \pm 0.018$	$0.796 \pm 0.019$	$0.867 \pm 0.044$	$0.862 \pm 0.043$	$0.843 \pm 0.021$
EnD <sup>2</sup> , $T = 10.0$		$0.792 \pm 0.012$	$0.805 \pm 0.013$	<b><math>0.886 \pm 0.009</math></b>	$0.873 \pm 0.009$	$0.849 \pm 0.013$
Single	LSN-C	$0.864 \pm 0.044$	$0.864 \pm 0.044$	-	-	-
ENSM		-	$0.902 \pm \text{NA}$	-	$0.703 \pm \text{NA}$	$0.896 \pm \text{NA}$
EnD		$0.730 \pm 0.019$	$0.730 \pm 0.019$	-	-	-
EnD <sup>2</sup> , $T = 1.0$		$0.894 \pm 0.043$	$0.906 \pm 0.039$	$0.966 \pm 0.019$	$0.958 \pm 0.019$	$0.944 \pm 0.029$
EnD <sup>2</sup> , $T = 10.0$		$0.932 \pm 0.014$	$0.941 \pm 0.013$	<b><math>0.983 \pm 0.006</math></b>	$0.972 \pm 0.007$	$0.967 \pm 0.009$
Single	KITTI	$0.947 \pm 0.023$	$0.947 \pm 0.023$	-	-	-
ENSM		-	$0.969 \pm \text{NA}$	-	$0.865 \pm \text{NA}$	$0.970 \pm \text{NA}$
EnD		$0.868 \pm 0.022$	$0.868 \pm 0.022$	-	-	-
EnD <sup>2</sup> , $T = 1.0$		$0.914 \pm 0.043$	$0.922 \pm 0.042$	$0.937 \pm 0.026$	$0.937 \pm 0.023$	$0.947 \pm 0.036$
EnD <sup>2</sup> , $T = 10.0$		$0.947 \pm 0.008$	$0.954 \pm 0.008$	$0.961 \pm 0.006$	$0.957 \pm 0.006$	<b><math>0.972 \pm 0.005</math></b>

## 6 Conclusion

The current work extends Prior Networks to regression tasks. Specifically, a regression Prior Network yields the parameters of the formidable Normal-Wishart distribution, which enables it to emulate ensembles of regression models and yield probabilistically meaningful measures of uncertainty at low computational cost. In this work measures of *total*, *data* and *knowledge uncertainty* were obtained for Normal-Wishart Regression Prior Networks in closed form. Two training approaches were proposed. First, the reverse-KL divergence between the model and a target Normal-Wishart distribution. This objective allows the behaviour of a Prior Network to be explicitly controlled, but requires an OOD training dataset. Second, via Ensemble Distribution Distillation (EnD<sup>2</sup>), where an ensemble of regression models is distilled into a Prior Networks such that it retains the improved predictive performance and robust uncertainty estimates of the original ensemble. This is particularly useful when it is challenging to define an out-of-domain training dataset. The properties of Regression Prior Networks were validated on a synthetic dataset and selected UCI datasets, where it was shown that they perform comparably to state-of-the-art ensemble approaches. Furthermore, the value of Ensemble Distribution Distillation was demonstrated on a large-scale monocular depth-estimation task. Here, an ensemble of probabilistic depth-estimation models was distribution-distilled into a Prior Network model. The resulting model retained both the improved predictive performance and uncertainty measures of an ensemble. Interestingly, due to the Prior Network over-estimating the support of the ensemble’s distribution, it is in fact better calibrated and yields superior out-of-domain detection results. To summarise, the current work yields a new set of efficient and interpretable uncertainty estimation approaches which can be applied to any regression task.

## Broader Impact

Predictive uncertainty estimation enables the safe and robust deployment of machine learning solutions, especially in high risk applications, such as finance or self-driving cars. Crucially, not only should uncertainty estimation techniques be interpretable and accurate, they should also be computationally efficient. Most modern approaches to uncertainty are based on ensemble techniques. These schemes yield robust and calibrated uncertainty estimates and improves predictive performance. Unfortunately the computational cost at inference time scales linearly with the size of the ensemble, making them poorly suited to resource-limited applications such as self driving cars. To address the problem, this paper proposes a significant extension to the existing prior network framework that enables uncertainty approaches to be efficiently applied to regression tasks. These regression prior networks maintain the uncertainty interpretability of ensemble approaches, with the efficiency of a single model, increasing the range of domains in which uncertainty approaches can be applied. Given the importance of uncertainty approaches to a wide-range of machine learning applications, this is a significant contribution to the community.

## References

- [1] Ross Girshick, “Fast R-CNN,” in *Proc. 2015 IEEE International Conference on Computer Vision (ICCV)*, 2015, pp. 1440–1448.
- [2] Karen Simonyan and Andrew Zisserman, “Very Deep Convolutional Networks for Large-Scale Image Recognition,” in *Proc. International Conference on Learning Representations (ICLR)*, 2015.
- [3] Ruben Villegas, Jimei Yang, Yuliang Zou, Sungryull Sohn, Xunyu Lin, and Honglak Lee, “Learning to Generate Long-term Future via Hierarchical Prediction,” in *Proc. International Conference on Machine Learning (ICML)*, 2017.
- [4] Tomas Mikolov et al., “Linguistic Regularities in Continuous Space Word Representations,” in *Proc. NAACL-HLT*, 2013.
- [5] Tomas Mikolov, Kai Chen, Greg Corrado, and Jeffrey Dean, “Efficient Estimation of Word Representations in Vector Space,” <http://arxiv.org/abs/1301.3781>, 2013, arXiv:1301.3781.
- [6] Tomas Mikolov, Martin Karafiát, Lukás Burget, Jan Cernocký, and Sanjeev Khudanpur, “Re-current Neural Network Based Language Model,” in *Proc. INTERSPEECH*, 2010.
- [7] Geoffrey Hinton, Li Deng, Dong Yu, George Dahl, Abdel rahman Mohamed, Navdeep Jaitly, Andrew Senior, Vincent Vanhoucke, Patrick Nguyen, Tara Sainath, and Brian Kingsbury, “Deep neural networks for acoustic modeling in speech recognition,” *Signal Processing Magazine*, 2012.
- [8] Awni Y. Hannun, Carl Case, Jared Casper, Bryan Catanzaro, Greg Diamos, Erich Elsen, Ryan Prenger, Sanjeev Satheesh, Shubho Sengupta, Adam Coates, and Andrew Y. Ng, “Deep speech: Scaling up end-to-end speech recognition,” 2014, arXiv:1412.5567.
- [9] Rich Caruana, Yin Lou, Johannes Gehrke, Paul Koch, Marc Sturm, and Noemie Elhadad, “Intelligible models for healthcare: Predicting pneumonia risk and hospital 30-day readmission,” in *Proc. 21th ACM SIGKDD International Conference on Knowledge Discovery and Data Mining*, New York, NY, USA, 2015, KDD ’15, pp. 1721–1730, ACM.
- [10] Babak Alipanahi, Andrew DeLong, Matthew T. Weirauch, and Brendan J. Frey, “Predicting the sequence specificities of DNA- and RNA-binding proteins by deep learning,” *Nature Biotechnology*, vol. 33, no. 8, pp. 831–838, July 2015.
- [11] Dario Amodei, Chris Olah, Jacob Steinhardt, Paul F. Christiano, John Schulman, and Dan Mané, “Concrete problems in AI safety,” <http://arxiv.org/abs/1606.06565>, 2016, arXiv:1606.06565.
- [12] Yarin Gal and Zoubin Ghahramani, “Dropout as a Bayesian Approximation: Representing Model Uncertainty in Deep Learning,” in *Proc. 33rd International Conference on Machine Learning (ICML-16)*, 2016.

- [13] B. Lakshminarayanan, A. Pritzel, and C. Blundell, “Simple and Scalable Predictive Uncertainty Estimation using Deep Ensembles,” in *Proc. Conference on Neural Information Processing Systems (NIPS)*, 2017.
- [14] Wesley Maddox, Timur Garipov, Pavel Izmailov, Dmitry Vetrov, and Andrew Gordon Wilson, “A simple baseline for bayesian uncertainty in deep learning,” *arXiv preprint arXiv:1902.02476*, 2019.
- [15] Andrey Malinin, *Uncertainty Estimation in Deep Learning with application to Spoken Language Assessment*, Ph.D. thesis, University of Cambridge, 2019.
- [16] Nicholas Carlini and David A. Wagner, “Adversarial examples are not easily detected: Bypassing ten detection methods,” *CoRR*, 2017.
- [17] L. Smith and Y. Gal, “Understanding Measures of Uncertainty for Adversarial Example Detection,” in *UAI*, 2018.
- [18] Andreas Kirsch, Joost van Amersfoort, and Yarin Gal, “Batchbald: Efficient and diverse batch acquisition for deep bayesian active learning,” 2019.
- [19] Andrey Malinin and Mark Gales, “Predictive uncertainty estimation via prior networks,” in *Advances in Neural Information Processing Systems*, 2018, pp. 7047–7058.
- [20] Andrey Malinin and Mark JF Gales, “Reverse kl-divergence training of prior networks: Improved uncertainty and adversarial robustness,” 2019.
- [21] Andrey Malinin, Bruno Mlodozieniec, and Mark JF Gales, “Ensemble distribution distillation,” in *International Conference on Learning Representations*, 2020.
- [22] Christopher M Bishop, *Pattern recognition and machine learning*, springer, 2006.
- [23] Ian Goodfellow, Yoshua Bengio, and Aaron Courville, *Deep learning*, MIT press, 2016.
- [24] Kevin P. Murphy, *Machine Learning*, The MIT Press, 2012.
- [25] Arsenii Ashukha, Alexander Lyzhov, Dmitry Molchanov, and Dmitry Vetrov, “Pitfalls of in-domain uncertainty estimation and ensembling in deep learning,” in *International Conference on Learning Representations*, 2020.
- [26] Yaniv Ovadia, Emily Fertig, Jie Ren, Zachary Nado, D Sculley, Sebastian Nowozin, Joshua V Dillon, Balaji Lakshminarayanan, and Jasper Snoek, “Can you trust your model’s uncertainty? evaluating predictive uncertainty under dataset shift,” *Advances in Neural Information Processing Systems*, 2019.
- [27] Stanislav Fort, Huiyi Hu, and Balaji Lakshminarayanan, “Deep ensembles: A loss landscape perspective,” *arXiv preprint arXiv:1912.02757*, 2019.
- [28] Dan Hendrycks and Kevin Gimpel, “A Baseline for Detecting Misclassified and Out-of-Distribution Examples in Neural Networks,” <http://arxiv.org/abs/1610.02136>, 2016, arXiv:1610.02136.
- [29] Pushmeet Kohli Nathan Silberman, Derek Hoiem and Rob Fergus, “Indoor segmentation and support inference from rgb-d images,” in *ECCV*, 2012.
- [30] Ibraheem Alhashim and Peter Wonka, “High quality monocular depth estimation via transfer learning,” *arXiv e-prints*, vol. abs/1812.11941, 2018.
- [31] Moritz Menze and Andreas Geiger, “Object scene flow for autonomous vehicles,” in *Conference on Computer Vision and Pattern Recognition (CVPR)*, 2015.
- [32] Fisher Yu, Yinda Zhang, Shuran Song, Ari Seff, and Jianxiong Xiao, “LSUN: construction of a large-scale image dataset using deep learning with humans in the loop,” 2015, arXiv:1506.03365.
- [33] Maya Gupta and Santosh Srivastava, “Parametric bayesian estimation of differential entropy and relative entropy,” *Entropy*, vol. 12, no. 4, pp. 818–843, 2010.
- [34] Thomas M Cover and Joy A Thomas, *Elements of information theory*, John Wiley & Sons, 2006.
- [35] REINALDO B ARELLANO-VALLE, JAVIER E CONTRERAS-REYES, and Marc G Genton, “Shannon entropy and mutual information for multivariate skew-elliptical distributions,” *Scandinavian Journal of Statistics*, vol. 40, no. 1, pp. 42–62, 2013.

## A Derivations for Normal-Wishart Prior Networks

The current appendix provides mathematical details of the Normal-Wishart distribution and derivations of the reverse-KL divergence loss, ensemble distribution distillation and all uncertainty measures.

### A.1 Normal-Wishart distribution

The Normal-Wishart distribution is a conjugate prior over the mean  $\mu$  and precision  $\Lambda$  of a normal distribution, defined as follows

$$p(\mu, \Lambda | \Omega) = \mathcal{N}\mathcal{W}(\mu, \Lambda | \mathbf{m}, \mathbf{L}, \kappa, \nu) = \mathcal{N}(\mu | \mathbf{m}, \kappa \Lambda) \mathcal{W}(\Lambda | \mathbf{L}, \nu); \quad (16)$$

where  $\Omega = \{\mathbf{m}, \mathbf{L}, \kappa, \nu\}$  are the parameters predicted by neural network,  $\mathcal{N}$  is the density of the Normal and  $\mathcal{W}$  is the density of the Wishart distribution. Here,  $\mathbf{m}$  and  $\mathbf{L}$  are the *prior mean* and inverse of the positive-definite *prior scatter matrix*, while  $\kappa$  and  $\nu$  are the strengths of belief in each prior, respectively. The parameters  $\kappa$  and  $\nu$  are conceptually similar to *precision* of the Dirichlet distribution  $\alpha_0$ . The Normal-Wishart is a compound distribution which decomposes into a product of a conditional normal distribution over the mean and an Wishart distribution over the precision:

$$\begin{aligned} \mathcal{N}(\mu | \mathbf{m}, \kappa \Lambda) &= \frac{\kappa^{\frac{D}{2}} |\Lambda|^{\frac{1}{2}}}{2\pi^{\frac{D}{2}}} \exp\left(-\frac{\kappa}{2}(\mu - \mathbf{m})^T \Lambda (\mu - \mathbf{m})\right) \\ \mathcal{W}(\Lambda | \mathbf{L}, \nu) &= \frac{|\Lambda|^{\frac{\nu-K-1}{2}} \exp(-\frac{1}{2} \text{Tr}(\Lambda \mathbf{L}^{-1}))}{2^{\frac{\nu K}{2}} \Gamma_K(\frac{\nu}{2}) |\mathbf{L}|^{\frac{\nu}{2}}}; \quad \Lambda, \mathbf{L} \succ 0, \nu > K - 1. \end{aligned} \quad (17)$$

where  $\Gamma_K(\cdot)$  is the *multivariate gamma function* and  $K$  is the dimensionality of  $\mathbf{y}$ . From [24] the posterior predictive of this model is the multivariate T-distribution:

$$p(\mathbf{y} | \mathbf{x}, \theta) = \mathbb{E}_{p(\mu, \Lambda | \mathbf{x}, \theta)} [p(\mathbf{y} | \mu, \Lambda)] = \mathcal{T}(\mathbf{y} | \mathbf{m}, \frac{\kappa + 1}{\kappa(\nu - K + 1)} \mathbf{L}^{-1}, \nu - K + 1). \quad (18)$$

The  $\mathcal{T}$  distribution is heavy-tailed generalization of the multivariate normal distribution defined as:

$$\mathcal{T}(\mathbf{y} | \mu, \Sigma, \nu) = \frac{\Gamma(\frac{\nu+K}{2})}{\Gamma(\frac{\nu}{2}) \nu^{\frac{K}{2}} \pi^{\frac{K}{2}} |\Sigma|^{\frac{1}{2}}} \left(1 + \frac{1}{\nu} (\mathbf{y} - \mu)^T \Sigma^{-1} (\mathbf{y} - \mu)\right)^{-\frac{(\nu+K)}{2}}, \quad \nu \geq 0; \quad (19)$$

where  $\nu$  is the number of degrees of freedom. However, the mean is only defined when  $\nu > 1$  and the variance is defined only when  $\nu > 2$ .

### A.2 Reverse KL-divergence Training Objective

Now let us consider in greater detail the reverse KL-divergence training objective (11):

$$\mathcal{L}(\mathbf{y}, \mathbf{x}, \theta; \hat{\beta}, \Omega_0) = \hat{\beta} \cdot \mathbb{E}_{p(\mu, \Lambda | \mathbf{x}, \theta)} [-\ln p(\mathbf{y} | \mu, \Lambda)] + \text{KL}[p(\mu, \Lambda | \mathbf{x}, \theta) \| p(\mu, \Lambda | \Omega_0)] + Z \quad (20)$$

where  $\Omega_0 = [\mathbf{m}_0, \mathbf{L}_0, \kappa_0, \nu_0]$  are prior parameters that we set manually as discussed in section 2.2. It is necessary to show why the reverse KL-divergence objective will yield the correct level of data uncertainty. Lets consider taking the expectation of the first term in (11) with respect to the *true distribution* of targets  $p_{tr}(\mathbf{y} | \mathbf{x})$ . Trivially, we can show that by exchanging the order of expectation, that we are optimizing the expected cross-entropy between samples from the Normal-Wishart and the true distribution:

$$\mathbb{E}_{p_{tr}(\mathbf{y} | \mathbf{x})} [\mathbb{E}_{p(\mu, \Lambda | \mathbf{x}, \theta)} [-\ln p(\mathbf{y} | \mu, \Lambda)]] = \mathbb{E}_{p(\mu, \Lambda | \mathbf{x}, \theta)} [\mathbb{E}_{p_{tr}(\mathbf{y} | \mathbf{x})} [-\ln p(\mathbf{y} | \mu, \Lambda)]] \quad (21)$$

This will yield an upper bound on the cross entropy between the predictive posterior and the true distribution. However, if we were to consider the *forward* KL-divergence between Normal-Wishart distributions, we would not obtain such an expression and not correctly estimate data uncertainty. Interestingly, the reverse KL-divergence training objective has the same form as an ELBO - the predictive term and a reverse KL-divergence to the prior.

Having established an important property of the RKL objective, we not derive it's closed form expression. Note, that in these derivations, we make extended use of properties for taking expectations

of traces and log-determinants matrices with respect to the Wishart distribution detailed in [33]. For the first term in 20, we use the following property of the multivariate normal:

$$x \sim \mathcal{N}(\boldsymbol{\mu}, \boldsymbol{\Sigma}) \Rightarrow \mathbb{E}[x^T \mathbf{A} x] = \text{Tr}(\mathbf{A} \boldsymbol{\Sigma}) + \mathbf{m}^T \mathbf{A} \mathbf{m}; \quad (22)$$

which allows us to get:

$$\begin{aligned} & \mathbb{E}_{\mathbf{p}(\boldsymbol{\mu}, \boldsymbol{\Lambda} | \mathbf{x}; \boldsymbol{\theta})} [-\ln \mathbf{p}(\mathbf{y} | \boldsymbol{\mu}, \boldsymbol{\Lambda})] = \\ &= \frac{1}{2} \mathbb{E}_{\mathbf{p}(\boldsymbol{\mu}, \boldsymbol{\Lambda} | \mathbf{x}; \boldsymbol{\theta})} [(\mathbf{y} - \boldsymbol{\mu})^T \boldsymbol{\Lambda} (\mathbf{y} - \boldsymbol{\mu}) + K \ln(2\pi) - \ln |\boldsymbol{\Lambda}|] \\ &= \frac{1}{2} \mathbb{E}_{\mathcal{N}(\boldsymbol{\mu} | \mathbf{m}, \kappa \boldsymbol{\Lambda}) \mathcal{W}(\boldsymbol{\Lambda} | \mathbf{L}, \nu)} [(\mathbf{y} - \boldsymbol{\mu})^T \boldsymbol{\Lambda} (\mathbf{y} - \boldsymbol{\mu}) + K \ln(2\pi) - \ln |\boldsymbol{\Lambda}|] \\ &\propto \frac{1}{2} \mathbb{E}_{\mathbf{p}(\boldsymbol{\Lambda} | \mathbf{L}; \nu)} [(\mathbf{y} - \mathbf{m})^T \boldsymbol{\Lambda} (\mathbf{y} - \mathbf{m}) + K \kappa^{-1} - \ln |\boldsymbol{\Lambda}|] \\ &= \frac{\nu}{2} (\mathbf{y} - \mathbf{m})^T \mathbf{L} (\mathbf{y} - \mathbf{m}) + \frac{K}{2\kappa} - \frac{1}{2} \ln |\mathbf{L}| - \frac{1}{2} \psi_K\left(\frac{\nu}{2}\right) + \frac{K}{2} \ln \pi. \end{aligned} \quad (23)$$

The second term in (20) may expressed as follows via the chain-rule of relative entropy [34]:

$$\begin{aligned} & \text{KL}[\mathbf{p}(\boldsymbol{\mu}, \boldsymbol{\Lambda} | \boldsymbol{\Omega}) \| \mathbf{p}(\boldsymbol{\mu}, \boldsymbol{\Lambda} | \boldsymbol{\Omega}_0)] = \\ &= \mathbb{E}_{\mathbf{p}(\boldsymbol{\Lambda} | \boldsymbol{\Omega})} [\text{KL}[\mathbf{p}(\boldsymbol{\mu} | \boldsymbol{\Lambda}, \boldsymbol{\Omega}) \| \mathbf{p}(\boldsymbol{\mu} | \boldsymbol{\Lambda}, \boldsymbol{\Omega}_0)]] + \text{KL}[\mathbf{p}(\boldsymbol{\Lambda} | \boldsymbol{\Omega}) \| \mathbf{p}(\boldsymbol{\Lambda} | \boldsymbol{\Omega}_0)]; \end{aligned} \quad (24)$$

The first term in (24) can be computed as:

$$\begin{aligned} & \mathbb{E}_{\mathbf{p}(\boldsymbol{\Lambda} | \boldsymbol{\Omega})} [\text{KL}[\mathbf{p}(\boldsymbol{\mu} | \boldsymbol{\Lambda}, \boldsymbol{\Omega}) \| \mathbf{p}(\boldsymbol{\mu} | \boldsymbol{\Lambda}, \boldsymbol{\Omega}_0)]] = \\ &= \mathbb{E}_{\mathcal{W}(\boldsymbol{\Lambda} | \mathbf{L}, \nu)} [\text{KL}[\mathcal{N}(\mathbf{y} | \mathbf{m}, \kappa \boldsymbol{\Lambda}) \| \mathcal{N}(\mathbf{y} | \mathbf{m}_0, \kappa_0 \boldsymbol{\Lambda})]] \\ &= \frac{\kappa_0}{2} (\mathbf{m} - \mathbf{m}_0)^T \nu \mathbf{L} (\mathbf{m} - \mathbf{m}_0) + \frac{K}{2} \left( \frac{\kappa_0}{\kappa} - \ln \frac{\kappa_0}{\kappa} - 1 \right); \end{aligned} \quad (25)$$

while the second term is:

$$\begin{aligned} & \text{KL}[\mathbf{p}(\boldsymbol{\Lambda} | \boldsymbol{\Omega}) \| \mathbf{p}(\boldsymbol{\Lambda} | \boldsymbol{\Omega}_0)] = \text{KL}[\mathcal{W}(\boldsymbol{\Lambda} | \mathbf{L}, \nu) \| \mathcal{W}(\boldsymbol{\Lambda} | \mathbf{L}_0, \nu_0)] = \\ &= \frac{\nu}{2} (\text{tr}(\mathbf{L}_0^{-1} \mathbf{L}) - K) - \frac{\nu_0}{2} \ln |\mathbf{L}_0^{-1} \mathbf{L}| + \ln \frac{\Gamma_K(\frac{\nu_0}{2})}{\Gamma_K(\frac{\nu}{2})} + \frac{\nu - \nu_0}{2} \psi_K\left(\frac{\nu}{2}\right). \end{aligned} \quad (26)$$

### A.3 Uncertainty Measures

Given a Normal-Wishart Prior Network which displays the desired set of behaviours detailed in 2, it is possible to compute closed-form expression for all measures of uncertainty previously discussed for Dirichlet Prior Networks [15]. The current section details the derivations of uncertainty measures introduced in section 2.1 for the Normal-Wishart distribution. We make extensive use of [33] for taking expectation of log-determinants and traces of matrices.

#### A.3.1 Differential Entropy of Predictive Posterior

As discussed in section 2, the predictive posterior of a Prior Network which parameterizes a Normal-Wishart distribution is a multivariate T distribution:

$$\mathbb{E}_{\mathbf{p}(\boldsymbol{\mu}, \boldsymbol{\Lambda} | \mathbf{x}; \boldsymbol{\theta})} [\mathbf{p}(\mathbf{y} | \boldsymbol{\mu}, \boldsymbol{\Lambda})] = \mathcal{T}(\mathbf{y} | \mathbf{m}, \frac{\kappa + 1}{\kappa(\nu - K + 1)} \mathbf{L}^{-1}, \nu - K + 1). \quad (27)$$

The differential entropy of the predictive posterior will be a measure of *total uncertainty*. The differential entropy of a standard multivariate student's T distribution with an identity scatter matrix  $\boldsymbol{\Sigma} = \mathbf{I}$  is given by:

$$\mathcal{H}[\mathcal{T}(\mathbf{x} | \boldsymbol{\mu}, \mathbf{I}, \nu)] = -\ln \frac{\Gamma(\frac{\nu+K}{2})}{\Gamma(\frac{\nu}{2})(\nu\pi)^{\frac{K}{2}}} + \left(\frac{\nu+K}{2}\right) \cdot \left(\psi\left(\frac{\nu+K}{2}\right) - \psi\left(\frac{\nu}{2}\right)\right); \quad (28)$$

which is a result obtained from [35]. Using the property of differential entropy [34], that if  $\mathbf{x} \sim \mathbf{p}(\mathbf{x})$  and  $\mathbf{y} = \boldsymbol{\mu} + \mathbf{A}\mathbf{x}$ , then:

$$\mathcal{H}[\mathbf{p}(\mathbf{y})] = \mathcal{H}[\mathbf{p}(\mathbf{x})] + \ln |\mathbf{A}|. \quad (29)$$

We can show that the differential entropy of a standard general multivariate student's T distribution is given by:

$$\mathcal{H}[\mathcal{T}(\mathbf{x}|\boldsymbol{\mu}, \boldsymbol{\Sigma}, \nu)] = \frac{1}{2} \ln |\boldsymbol{\Sigma}| - \ln \frac{\Gamma(\frac{\nu+K}{2})}{\Gamma(\frac{\nu}{2})(\nu\pi)^{\frac{K}{2}}} + (\frac{\nu+K}{2}) \cdot (\psi(\frac{\nu+K}{2}) - \psi(\frac{\nu}{2})). \quad (30)$$

Using this expression, we can show that the differential entropy of the predictive posterior of a Normal-Wishart Prior Network is given by:

$$\begin{aligned} \mathcal{H}[\mathbb{E}_{\mathbf{p}(\boldsymbol{\mu}, \boldsymbol{\Lambda}|\mathbf{x}, \boldsymbol{\theta})}[\mathbf{p}(\mathbf{y}|\boldsymbol{\mu}, \boldsymbol{\Lambda})]] &= \mathcal{H}[\mathcal{T}(\mathbf{y}|\mathbf{m}, \frac{\kappa+1}{\kappa(\nu-K+1)}\mathbf{L}^{-1}, \nu-K+1)] \\ &= \frac{\nu+1}{2} \left( \psi(\frac{\nu+1}{2}) - \psi(\frac{\nu-K+1}{2}) \right) - \ln \frac{\Gamma(\frac{\nu+1}{2})}{\Gamma(\frac{\nu-K+1}{2})((\nu-K+1)\pi)^{\frac{K}{2}}} \\ &\quad - \frac{1}{2} \ln |\mathbf{L}| + \frac{K}{2} \ln \frac{\kappa+1}{\kappa(\nu-K+1)}. \end{aligned} \quad (31)$$

### A.3.2 Mutual Information

The mutual information between the target  $\mathbf{y}$  and the parameters of the output distribution  $\{\boldsymbol{\mu}, \boldsymbol{\Lambda}\}$  is measures of *knowledge uncertainty*, and it the difference between the (differential) entropy of the predictive posterior and the expected differential entropy of each normal distribution sampled from the Normal Wishart:

$$\underbrace{\mathcal{I}[\mathbf{y}, \{\boldsymbol{\mu}, \boldsymbol{\Lambda}\}]}_{\text{Knowledge Uncertainty}} = \underbrace{\mathcal{H}[\mathbb{E}_{\mathbf{p}(\boldsymbol{\mu}, \boldsymbol{\Lambda}|\mathbf{x}, \boldsymbol{\theta})}[\mathbf{p}(\mathbf{y}|\boldsymbol{\mu}, \boldsymbol{\Lambda})]]}_{\text{Total Uncertainty}} - \underbrace{\mathbb{E}_{\mathbf{p}(\boldsymbol{\mu}, \boldsymbol{\Lambda}|\mathbf{x}, \boldsymbol{\theta})}[\mathcal{H}[\mathbf{p}(\mathbf{y}|\boldsymbol{\mu}, \boldsymbol{\Lambda})]]}_{\text{Expected Data Uncertainty}} \quad (32)$$

The first term, the differential entropy of the predictive posterior was derived above in (31). We we derive the expected differential entropy as follows:

$$\begin{aligned} \mathbb{E}_{\mathcal{NW}(\boldsymbol{\mu}, \boldsymbol{\Lambda}|\Omega)}[\mathcal{H}[\mathcal{N}(\mathbf{y}|\boldsymbol{\mu}, \boldsymbol{\Lambda})]] &= \frac{1}{2} \mathbb{E}_{\mathcal{NW}(\boldsymbol{\mu}, \boldsymbol{\Lambda}|\Omega)}[K \ln(2\pi e) - \ln |\boldsymbol{\Lambda}|] = \\ &= \frac{1}{2} [K \ln(\pi e) - \ln |\mathbf{L}| - \psi_K(\frac{\nu}{2})]. \end{aligned} \quad (33)$$

Thus, the final expression for mutual information is:

$$\begin{aligned} \mathcal{I}[\mathbf{y}, \{\boldsymbol{\mu}, \boldsymbol{\Lambda}\}] &= \frac{\nu+1}{2} \left( \psi(\frac{\nu+1}{2}) - \psi(\frac{\nu-K+1}{2}) \right) - \ln \frac{\Gamma(\frac{\nu+1}{2})}{\Gamma(\frac{\nu-K+1}{2})((\nu-K+1)\pi)^{\frac{K}{2}}} \\ &\quad + \frac{K}{2} \ln \frac{\kappa+1}{\kappa(\nu-K+1)} - \frac{1}{2} [K \ln(\pi e) - \psi_K(\frac{\nu}{2})]. \end{aligned} \quad (34)$$

Note that this expression is no longer a function of  $\mathbf{L}$ , which was important in representation *data uncertainty*.

### A.3.3 Expected Pairwise KL-Divergence

An alternative measures of *knowledge uncertainty* which can be considered is the expected pairwise kl-divergence (EPKL), which upper bounds mutual information [15]. In this section we derive it's closed form expression for the Normal-Wishart distribution.

$$\begin{aligned} \mathcal{K}[\mathbf{y}, \{\boldsymbol{\mu}, \boldsymbol{\Lambda}\}] &= \mathbb{E}_{\mathbf{p}(\boldsymbol{\mu}_0, \boldsymbol{\Lambda}_0)} \mathbb{E}_{\mathbf{p}(\boldsymbol{\mu}_1, \boldsymbol{\Lambda}_1)} [\text{KL}[\mathcal{N}(\mathbf{y}|\boldsymbol{\mu}_1, \boldsymbol{\Lambda}_1) \parallel \mathcal{N}(\mathbf{y}|\boldsymbol{\mu}_0, \boldsymbol{\Lambda}_0)]] \\ &= \frac{1}{2} \mathbb{E}_{\mathbf{p}(\boldsymbol{\mu}_0, \boldsymbol{\Lambda}_0)} \mathbb{E}_{\mathbf{p}(\boldsymbol{\mu}_1, \boldsymbol{\Lambda}_1)} \left[ (\boldsymbol{\mu}_1 - \boldsymbol{\mu}_0)^T \boldsymbol{\Lambda}_0 (\boldsymbol{\mu}_1 - \boldsymbol{\mu}_0) + \ln \frac{|\boldsymbol{\Lambda}_1|}{|\boldsymbol{\Lambda}_0|} + \text{Tr}(\boldsymbol{\Lambda}_0 \boldsymbol{\Lambda}_1^{-1}) - K \right]. \end{aligned} \quad (35)$$

Here  $p(\mu_0, \Lambda_0) = p(\mu_1, \Lambda_1) = p(\mu, \Lambda|x; \theta)$ . In (35) the first term is:

$$\begin{aligned} & \mathbb{E}_{p(\mu_0, \Lambda_0)} \mathbb{E}_{p(\mu_1, \Lambda_1)} [(\mu_1 - \mu_0)^T \Lambda_0 (\mu_1 - \mu_0)] = \\ &= \mathbb{E}_{p(\mu_0, \Lambda_0)} \mathbb{E}_{p(\Lambda_1)} [(\mathbf{m} - \mu_0)^T \Lambda_0 (\mathbf{m} - \mu_0) + \text{Tr}(\Lambda_0 \frac{1}{\kappa} \Lambda_1^{-1})] \\ &= \mathbb{E}_{p(\mu_0, \Lambda_0)} \left[ (\mathbf{m} - \mu_0)^T \Lambda_0 (\mathbf{m} - \mu_0) + \frac{1}{\kappa(\nu - K - 1)} \text{Tr}(\Lambda_0 L^{-1}) \right] \\ &= \frac{K}{\kappa} + \frac{\nu K}{\kappa(\nu - K - 1)}; \end{aligned} \quad (36)$$

The second term in (35) is zero, and the third term is:

$$\mathbb{E}_{p(\mu_0, \Lambda_0)} \mathbb{E}_{p(\mu_1, \Lambda_1)} [\text{Tr}(\Lambda_0 \Lambda_1^{-1})] = \mathbb{E}_{p(\mu_0, \Lambda_0)} \left[ \text{Tr}(\Lambda_0 \frac{1}{\nu - K - 1} L^{-1}) \right] = \frac{\nu K}{(\nu - K - 1)}; \quad (37)$$

which in sum gives us:

$$\mathcal{K}[\mathbf{y}, \{\mu, \Lambda\}] = \frac{1}{2} \frac{\nu K(\kappa^{-1} + 1)}{(\nu - K - 1)} - \frac{K}{2} + \frac{K}{2\kappa}. \quad (38)$$

Note that this is also not a function of  $\mathbf{L}$ , just like mutual information. Rather, it is only a function of the pseudo-counts  $\kappa$  and  $\nu$ .

### A.3.4 Law of Total Variation

Finally, in order to be able to compare with ensembles, we can also derive variance-based measures of *total*, *data* and *knowledge uncertainty* via the Law of total variance, as follows:

$$\underbrace{\mathbb{V}_{p(\mu, \Lambda|x, \theta)}[\mu]}_{\text{Knowledge Uncertainty}} = \underbrace{\mathbb{V}_{p(\mathbf{y}|x, \theta)}[\mathbf{y}]}_{\text{Total Uncertainty}} - \underbrace{\mathbb{E}_{p(\mu, \Lambda|x, \theta)}[\Lambda^{-1}]}_{\text{Expected Data Uncertainty}} \quad (39)$$

This has a similar decomposition as mutual information. In this section we derive its closed form expression. We can compute the expected variance by using the probabilistic change of variables:

$$\begin{aligned} \mathbb{E}_{p(\mu, \Lambda|x, \theta)}[\Lambda^{-1}] &= \mathbb{E}_{\mathcal{N}\mathcal{W}(\mu, \Lambda)}[\Lambda^{-1}] = \mathbb{E}_{\mathcal{W}(\Lambda)}[\Lambda^{-1}] = \mathbb{E}_{\mathcal{W}^{-1}(\Lambda^{-1})}[\Lambda^{-1}] \\ &= \frac{1}{\nu - K - 1} \mathbf{L}^{-1}; \end{aligned} \quad (40)$$

and the variance of expected as:

$$\begin{aligned} \mathbb{V}_{p(\mu, \Lambda|x, \theta)}[\mu] &= \mathbb{E}_{\mathcal{N}\mathcal{W}(\mu, \Lambda)}[(\mu - \mathbf{m})(\mu - \mathbf{m})^T] = \frac{1}{\kappa} \mathbb{E}_{\mathcal{W}(\Lambda|\mathbf{L}, \nu)}[\Lambda^{-1}] \\ &= \frac{1}{\kappa(\nu - K - 1)} \mathbf{L}^{-1}. \end{aligned} \quad (41)$$

Thus, the total variance is then expressed as:

$$\mathbb{V}_{p(\mathbf{y}|x, \theta)}[\mathbf{y}] = \frac{1 + \kappa}{\kappa(\nu - K - 1)} \mathbf{L}^{-1}. \quad (42)$$

Note that this yields a measure which only considers first and second moments. In addition, in order to obtain a scalar estimate of uncertainty, it is necessary to consider the log-determinant of each measure.

## B Experiment on Synthetic Data

The training data consists of 2048 inputs  $x$  uniformly sampled from  $[-10, 10]$  with targets  $y \sim \mathcal{N}(\sin x + \frac{x}{10})$ . We use a relu network with 2 hidden layers containing 30 units each to predict the parameters of either Gaussian or Normal-Wishart distribution on this data. In all cases, we use Adam optimizer with learning rate  $10^{-2}$  and weight decay  $10^{-4}$  for 800 epochs with batch size 128. Gaussian models in an ensemble are trained via negative log-likelihood starting from different random initialization. To train a Regression Prior Network with reverse-KL divergence 512 points were uniformly sampled from  $[-25, -20] \cup [20, 25]$  as training-ood data. We use objective (8) with coefficient  $\gamma = 0.5$ . The prior belief is  $\kappa_0 = 10^{-2}$  and in-domain  $\hat{\beta}$  is  $10^2$ . For EnD<sup>2</sup> training we set  $T = 1$  and add gaussian noise to inputs with standard deviation 3.

## C UCI Experiments

The current appendix provides additional details of experiments on the UCI regression datasets. Note that we leave out the Yacht Hydrodynamics datasets, as it is the smallest with the fewest features. The remaining datasets are described in the table below:

Table 5: Description of UCI datasets.

Dataset	size	number of features
Boston housing	506	13
Concrete Compressive Strength	1030	8
Energy efficiency	768	9
Combined Cycle Power	9568	4
Red Wine Quality	1599	11
YearPredictionMSD	515345	90

### C.1 Creating out-of-domain data

Here we detail how OOD training data for reverse KL-divergence trained Prior Networks is created and how evaluation OOD data is created.

As reverse KL-divergence training of Prior Networks requires out-of-domain training examples, we use a factor analysis model to generate samples for this in the same way as was done in [15]. Specifically, we train a linear generative model that approximates inputs with  $\hat{x} \sim \mathcal{N}(\mu, WW^T + \Psi)$ , where  $[W, \mu, \Psi]$  are model parameters. In-domain training data is used to train this model. The out-of-domain training examples are then sampled from  $\mathcal{N}(\mu, 3WW^T + 3\Psi)$ , such that we are sampling further from the in-domain region.

To estimate quality of out-of-domain detection, we additionally create evaluation out-of-domain data from external UCI datasets: "Relative location of CT slices on axial axis Data Set" for MSD and "Condition Based Maintenance of Naval Propulsion Plants Data Set" for other datasets. We drop all constant columns in them and leave first  $K$  columns and first  $N$  rows, where  $K$  is a number of features and  $N$  is a number of test examples in a corresponding dataset. For each comparison, the out-of-domain datasets are normalized by the per-column mean and variance obtained on in-domain training data.

### C.2 Training

Following [13] in all experiments except MSD we use 1 layer relu neural network with 50 hidden units, for MSD we use 100 hidden units. We optimize weights with Adam for 100 epochs with batch size 32. All hyper-parameters, including learning rate, weight decay, RKL prior belief in train data  $\kappa_0$ , RKL ood coefficient  $\gamma$  and EnD<sup>2</sup> initial temperature  $T$  and noise level  $\varepsilon$  are set based on grid search, where we use equal computational budget in all models to ensure fair comparison. Additionally, we use 10 folds cross-validation and report standard deviation based on it.

### C.3 Results for all datasets

The current section provide a full set of predictive performance, error detection and OOD detection results on UCI datasets in tables 6-8, respectively. Results in table 6 show that all models achieve comparable performance, and that EnD<sup>2</sup> tends to come close to the ensemble. Table 7 shows the error detection performance of all models in terms of prediction-rejection ratio (% PRR) [15]. The results clearly show that measures of *total uncertainty* are useful in detecting errors, though it this is more challenging on some datasets. At the same time measures of *knowledge uncertainty* do significantly worse. Finally, table 8 shows the OOD detection performance in terms of % AUC-ROC. Here measures of *knowledge uncertainty* do far better. Notably, on the larger datasets EnD<sup>2</sup> comes closer to the performance of an ensemble.

Table 6: Prediction performance metrics of models on six UCI datasets.

Data	RMSE ( $\downarrow$ )				NLL ( $\downarrow$ )			
	Single	ENSM	EnD <sup>2</sup>	NWPN	Single	ENSM	EnD <sup>2</sup>	NWPN
boston	3.54 $\pm$ 0.32	<b>3.52 <math>\pm</math> 0.32</b>	3.64 $\pm$ 0.33	3.53 $\pm$ 0.31	2.58 $\pm$ 0.08	2.53 $\pm$ 0.07	2.5 $\pm$ 0.05	<b>2.47 <math>\pm</math> 0.04</b>
energy	1.83 $\pm$ 0.07	<b>1.79 <math>\pm</math> 0.07</b>	1.98 $\pm$ 0.05	1.83 $\pm$ 0.07	1.38 $\pm$ 0.04	<b>1.32 <math>\pm</math> 0.04</b>	1.72 $\pm$ 0.04	1.65 $\pm$ 0.08
concrete	5.66 $\pm$ 0.19	<b>5.24 <math>\pm</math> 0.18</b>	6.13 $\pm$ 0.18	5.77 $\pm$ 0.24	3.11 $\pm$ 0.08	<b>3.00 <math>\pm</math> 0.04</b>	3.13 $\pm$ 0.03	3.05 $\pm$ 0.03
wine	0.65 $\pm$ 0.01	<b>0.63 <math>\pm</math> 0.01</b>	<b>0.63 <math>\pm</math> 0.01</b>	<b>0.63 <math>\pm</math> 0.01</b>	1.24 $\pm$ 0.16	0.96 $\pm$ 0.03	<b>0.91 <math>\pm</math> 0.02</b>	0.93 $\pm$ 0.02
power	4.07 $\pm$ 0.07	<b>4.00 <math>\pm</math> 0.07</b>	4.06 $\pm$ 0.07	4.09 $\pm$ 0.07	2.82 $\pm$ 0.02	<b>2.79 <math>\pm</math> 0.02</b>	<b>2.79 <math>\pm</math> 0.01</b>	2.81 $\pm$ 0.01
MSD	9.08 $\pm$ 0.00	<b>8.92 <math>\pm</math> 0.00</b>	8.94 $\pm$ 0.00	9.07 $\pm$ 0.00	3.51 $\pm$ 0.00	<b>3.39 <math>\pm</math> 0.00</b>	<b>3.39 <math>\pm</math> 0.00</b>	3.41 $\pm$ 0.00

Table 7: PRR scores on all six UCI datasets.

Data	Model	$\mathcal{H}[\mathbb{E}]$	$\mathbb{V}[\mathbf{y}]$	$\mathcal{I}$	$\mathcal{K}$	$\mathbb{V}[\boldsymbol{\mu}]$
boston	ENSM	-	0.60 $\pm$ 0.07	-	-0.15 $\pm$ 0.07	0.41 $\pm$ 0.08
	EnD <sup>2</sup>	<b>0.61 <math>\pm</math> 0.07</b>	<b>0.61 <math>\pm</math> 0.07</b>	-0.02 $\pm$ 0.15	-0.02 $\pm$ 0.15	0.59 $\pm$ 0.06
	NWPN	0.54 $\pm$ 0.08	0.54 $\pm$ 0.08	-0.05 $\pm$ 0.09	-0.05 $\pm$ 0.09	0.49 $\pm$ 0.08
energy	ENSM	-	<b>0.90 <math>\pm</math> 0.01</b>	-	-0.80 $\pm$ 0.02	0.34 $\pm$ 0.09
	EnD <sup>2</sup>	0.83 $\pm$ 0.02	0.83 $\pm$ 0.02	-0.77 $\pm$ 0.03	-0.77 $\pm$ 0.03	0.60 $\pm$ 0.05
	NWPN	0.85 $\pm$ 0.02	0.85 $\pm$ 0.02	0.32 $\pm$ 0.11	0.32 $\pm$ 0.11	0.84 $\pm$ 0.02
concrete	ENSM	-	0.48 $\pm$ 0.05	-	0.01 $\pm$ 0.07	0.27 $\pm$ 0.06
	EnD <sup>2</sup>	0.50 $\pm$ 0.03	0.49 $\pm$ 0.03	0.05 $\pm$ 0.06	0.05 $\pm$ 0.06	0.44 $\pm$ 0.03
	NWPN	<b>0.54 <math>\pm</math> 0.03</b>	<b>0.54 <math>\pm</math> 0.03</b>	0.35 $\pm$ 0.04	0.35 $\pm$ 0.04	0.51 $\pm$ 0.03
wine	ENSM	-	<b>0.32 <math>\pm</math> 0.02</b>	-	0.10 $\pm$ 0.03	0.25 $\pm$ 0.04
	EnD <sup>2</sup>	0.30 $\pm$ 0.02	0.30 $\pm$ 0.02	0.06 $\pm$ 0.03	0.06 $\pm$ 0.03	0.30 $\pm$ 0.02
	NWPN	0.30 $\pm$ 0.03	0.30 $\pm$ 0.03	-0.19 $\pm$ 0.03	-0.19 $\pm$ 0.03	0.26 $\pm$ 0.04
power	ENSM	-	<b>0.23 <math>\pm</math> 0.01</b>	-	-0.01 $\pm$ 0.02	0.05 $\pm$ 0.02
	EnD <sup>2</sup>	<b>0.23 <math>\pm</math> 0.01</b>	<b>0.23 <math>\pm</math> 0.01</b>	-0.02 $\pm$ 0.03	-0.02 $\pm$ 0.03	0.15 $\pm$ 0.02
	NWPN	0.20 $\pm$ 0.02	0.20 $\pm$ 0.02	-0.03 $\pm$ 0.02	-0.03 $\pm$ 0.02	0.16 $\pm$ 0.01
msd	ENSM	-	<b>0.64 <math>\pm</math> 0.0</b>	-	0.07 $\pm$ 0.0	0.39 $\pm$ 0.0
	EnD <sup>2</sup>	0.63 $\pm$ 0.0	0.63 $\pm$ 0.0	0.04 $\pm$ 0.0	0.04 $\pm$ 0.0	0.59 $\pm$ 0.0
	NWPN	<b>0.64 <math>\pm</math> 0.0</b>	<b>0.64 <math>\pm</math> 0.0</b>	-0.20 $\pm$ 0.0	-0.20 $\pm$ 0.0	0.61 $\pm$ 0.0

Table 8: OOD Detection (ROC-AUC) of models on UCI datasets.

Data	Model	$\mathcal{H}[\mathbb{E}]$	$\mathbb{V}[\mathbf{y}]$	$\mathcal{I}$	$\mathcal{K}$	$\mathbb{V}[\boldsymbol{\mu}]$
boston	ENSM	-	0.75 $\pm$ 0.02	-	0.68 $\pm$ 0.02	<b>0.86 <math>\pm</math> 0.02</b>
	EnD <sup>2</sup>	0.75 $\pm$ 0.01	0.75 $\pm$ 0.01	0.63 $\pm$ 0.01	0.63 $\pm$ 0.01	0.76 $\pm$ 0.01
	NWPN	0.64 $\pm$ 0.02	0.65 $\pm$ 0.02	0.71 $\pm$ 0.01	0.71 $\pm$ 0.01	0.69 $\pm$ 0.01
energy	ENSM	-	0.76 $\pm$ 0.01	-	0.51 $\pm$ 0.03	<b>0.77 <math>\pm</math> 0.03</b>
	EnD <sup>2</sup>	0.61 $\pm$ 0.02	0.61 $\pm$ 0.02	0.57 $\pm$ 0.02	0.57 $\pm$ 0.02	0.63 $\pm$ 0.03
	NWPN	0.43 $\pm$ 0.02	0.43 $\pm$ 0.02	0.66 $\pm$ 0.01	0.66 $\pm$ 0.01	0.47 $\pm$ 0.02
concrete	ENSM	-	<b>0.84 <math>\pm</math> 0.01</b>	-	0.78 $\pm$ 0.02	0.82 $\pm$ 0.01
	EnD <sup>2</sup>	0.48 $\pm$ 0.02	0.48 $\pm$ 0.02	0.45 $\pm$ 0.01	0.45 $\pm$ 0.01	0.47 $\pm$ 0.01
	NWPN	<b>0.84 <math>\pm</math> 0.01</b>	<b>0.84 <math>\pm</math> 0.01</b>	0.8 $\pm$ 0.01	0.8 $\pm$ 0.01	0.83 $\pm$ 0.01
wine	ENSM	-	0.48 $\pm$ 0.03	-	0.58 $\pm$ 0.01	0.56 $\pm$ 0.02
	EnD <sup>2</sup>	0.59 $\pm$ 0.03	0.60 $\pm$ 0.03	<b>0.65 <math>\pm</math> 0.01</b>	<b>0.65 <math>\pm</math> 0.01</b>	<b>0.65 <math>\pm</math> 0.03</b>
	NWPN	0.42 $\pm$ 0.02	0.42 $\pm$ 0.02	0.64 $\pm$ 0.01	0.64 $\pm$ 0.01	0.53 $\pm$ 0.02
power	ENSM	-	0.35 $\pm$ 0.02	-	0.64 $\pm$ 0.02	0.62 $\pm$ 0.02
	EnD <sup>2</sup>	0.37 $\pm$ 0.03	0.37 $\pm$ 0.03	<b>0.66 <math>\pm</math> 0.01</b>	<b>0.66 <math>\pm</math> 0.01</b>	0.50 $\pm$ 0.02
	NWPN	0.24 $\pm$ 0.01	0.24 $\pm$ 0.01	0.56 $\pm$ 0.01	0.56 $\pm$ 0.01	0.31 $\pm$ 0.02
msd	ENSM	-	0.66 $\pm$ 0.0	-	0.55 $\pm$ 0.0	0.62 $\pm$ 0.0
	EnD <sup>2</sup>	0.66 $\pm$ 0.0	0.66 $\pm$ 0.0	0.50 $\pm$ 0.0	0.50 $\pm$ 0.0	0.65 $\pm$ 0.0
	NWPN	0.68 $\pm$ 0.0	0.68 $\pm$ 0.0	0.73 $\pm$ 0.0	0.73 $\pm$ 0.0	<b>0.75 <math>\pm</math> 0.0</b>

## D Nyu Depth Experiments

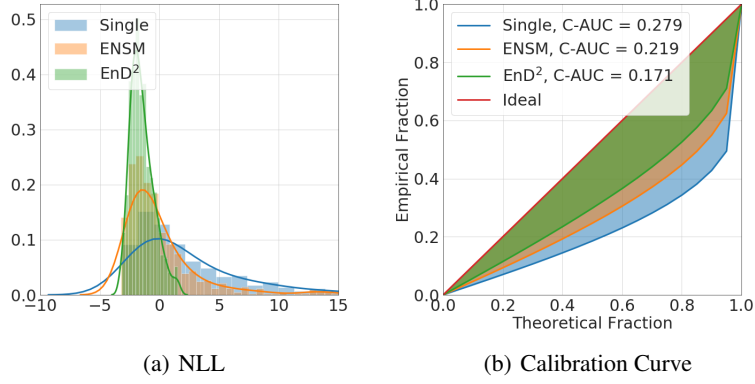


Figure 4: NLL histogram and calibration curve

Table 9 shows that EnD also has significantly worse calibration than even a single models, and the temperature annealing improves calibration, both in terms of NLL and C-AUC. The latter is the area between the calibration curve and the diagonal (C-AUC). A histogram of NLL and calibrations curves are provided in the figure below. We can see that EnD<sup>2</sup> yields far more consistent NLL, and has the best predictive intervals in terms of C-AUC, which is the area between the diagonal and the calibration curve. Note, that for all models we assume normally distributed predictive intervals, as was originally does in [13].

Table 9: Calibration performance comparison in terms of NLL and C-AUC

Method	NLL(↓)	C-AUC(↓)
ENSM 5	$0.76 \pm \text{NA}$	$0.219 \pm \text{NA}$
Single	$5.93 \pm 1.72$	$0.293 \pm 0.011$
EnD	$9.11 \pm 2.65$	$0.316 \pm 0.015$
EnD <sup>2</sup> , $T = 1.0$	$-1.43 \pm 0.02$	$0.178 \pm 0.008$
EnD <sup>2</sup> , $T = 10.0$	<b><math>-1.47 \pm 0.06</math></b>	<b><math>0.170 \pm 0.011</math></b>

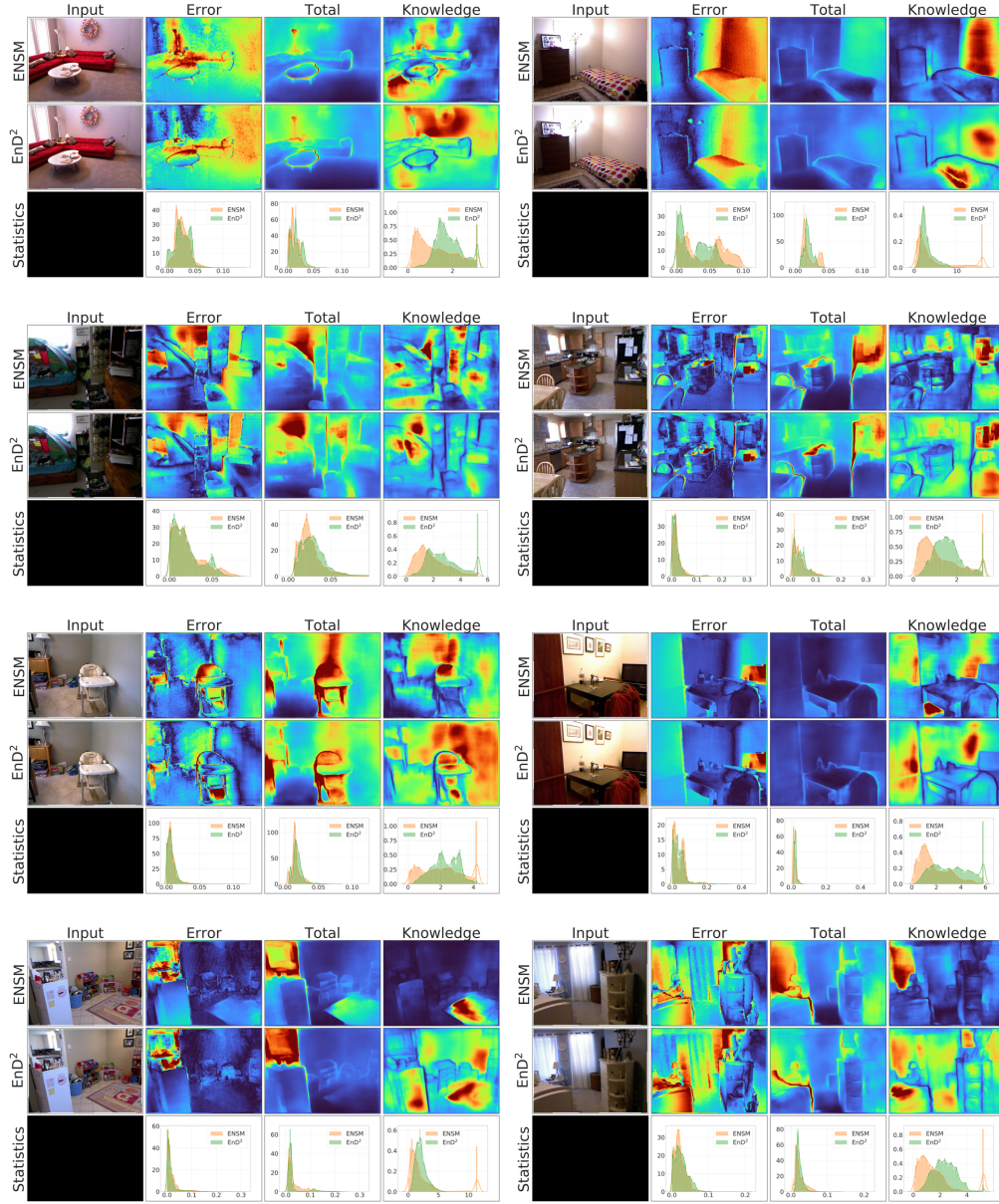


Figure 5: Uncurated comparison of ENSM vs End<sup>2</sup> behaviour on Nyuv2 dataset (best viewed in color).

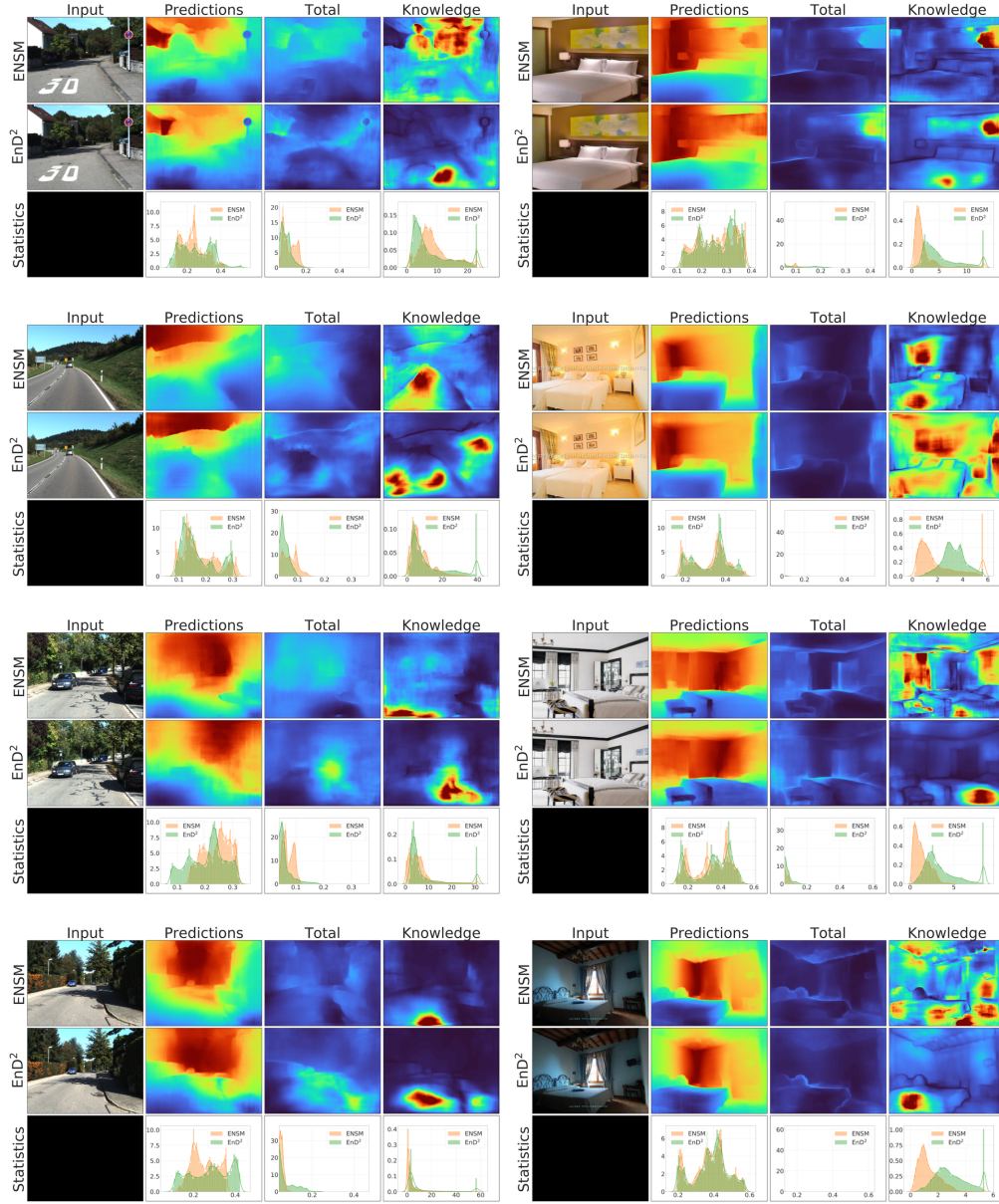


Figure 6: Uncurated comparison of ENSM vs EnD<sup>2</sup> models trained on Nyuv2 behaviour on Kitti and LSUN-bed datasets (best viewed in color).